Nuclear Engineering and Design 254 (2013) 237–245

Contents lists available at SciVerse ScienceDirect

Nuclear Engineering and Design

journal homepage: www.elsevier.com/locate/nucengdes

Integral transform solutions of dynamic response of a clamped–clamped pipe conveying fluid

Jijun Gu[a], Chen An[a], Menglan Duan[c], Carlos Levi[a], Jian Su[b,*]

[a] Ocean Engineering Program, COPPE, Universidade Federal do Rio de Janeiro, CP 68508, Rio de Janeiro 21941-972, Brazil
[b] Nuclear Engineering Program, COPPE, Universidade Federal do Rio de Janeiro, CP 68509, Rio de Janeiro 21941-972, Brazil
[c] Offshore Oil/Gas Research Center, China University of Petroleum, Beijing 102249, China

HIGHLIGHTS

- Dynamic response of pipe conveying fluid was studied numerically.
- The generalized integral transform technique (GITT) was applied.
- Numerical solutions with automatic global accuracy control were obtained.
- Excellent convergence behavior was shown.
- Modal separation analysis was carried out and the influence of mass ratio was analyzed.

ARTICLE INFO

Article history:
Received 4 January 2012
Received in revised form
11 September 2012
Accepted 30 September 2012

Keywords:
Pipe conveying fluid
Fluid–structure interaction
Internal fluid
Clamped–clamped pipe
Integral transform
Modal analysis

ABSTRACT

Analysis of dynamic response of pipe conveying fluid is an important aspect in nuclear power plant design. In the present paper, dynamic response of a clamped–clamped pipe conveying fluid was solved by the generalized integral transform technique (GITT). The governing partial differential equation was transformed into a set of second-order ordinary differential equations which is then numerically solved by making use of the subroutine DIVPAG from IMSL Library. A thorough convergence analysis was performed to yield sets of reference results of the transverse deflection at different time and spanwise position. We found good agreement between the computed natural frequencies at mode 1–3 and those obtained by previous theoretical study. Besides, modal separation analysis was carried out and the influence of mass ratio on deflection and natural frequencies was qualitatively and quantitatively assessed.

1. Introduction

Pipes conveying fluids are essential parts of a nuclear power plant. Flow-induced vibration of such pipes is a major concern for design, operation, maintenance, and safety analysis of a nuclear power plant. A fluid flowing in a pipe may exert forces on the pipe wall, deflect the pipe, cause vibration, and eventually result in long-term fatigue failures. Analysis of dynamic response of a pipe excited by internal flowing fluid is an important aspect in the design of nuclear power plants, since vibrations related to fluid–structure interaction may lead to pipe rupture and thus possible accidents. The main consideration might focus on the natural frequency and mode shapes of pipe, as well as the critical fluid velocity. The accurate prediction of natural frequencies and mode shapes of a pipe will help select the proper support locations, which could reduce the occurrence of fatigue-related pipe failures. Meanwhile, a critical fluid velocity will cause system instability, which would induce the pipes fail suddenly in a short time duration.

Various aspects of the dynamic characteristics of pipes conveying fluid have been extensively studied (Ibrahim, 2010, 2011), as well as cantilevered pipe conveying fluid (Païdoussis et al., 2002, 2007; Lopes et al., 2002; Semler et al., 2002; Wadham-Gagnon et al., 2007; Modarres-Sadeghi et al., 2007). In the nuclear engineering fields, Kang (2010) studied the effects of rotaty inertia of concentrated masses on the natural vibrations of a fluid-conveying pipe by theoretical modeling and numerical calculations. Sinha et al. (2005) derived a combination of a linear and a non-linear optimization methods for the prediction of the flow-induced excitation forces and the structural response at each measured frequency all along the pipe length. Huang et al. (2010) investigated the natural

* Corresponding author. Tel.: +55 21 2562 8448; fax: +55 21 2562 8444
E-mail addresses: sujian@nuclear.ufrj.br, sujian@lasme.coppe.ufrj.br (J. Su).

0029-5493/$ – see front matter © 2012 Elsevier B.V. All rights reserved.
http://dx.doi.org/10.1016/j.nucengdes.2012.09.018

Nomenclature

A_{ij}	integral transformation coefficient
B_{ij}	integral transformation coefficient
EI	flexural stiffness
f	dimensionless natural frequency
i	index
j	index
L	length of the pipe
m_f	mass of the fluid
m_p	mass of the pipe
N	truncation order
N_i	normalization integral
t	dimensionless time
T	time
u	dimensionless flow velocity
u_{cd}	dimensionless critical flow velocity
U	flow velocity
$\bar{y}$	transformed lateral deflection of the pipe
y	dimensionless lateral deflection of the pipe
Y	lateral deflection of the pipe
z	dimensionless axial coordinate
Z	axial coordinate

Greek symbols

β	mass ratio
δ	coefficient
λ	eigenvalue
ϕ	eigenfunction
$\tilde{\phi}$	normalized eigenfunction
ω	natural angular frequency

Acronyms

DTM	Differential Transformation Method
DQM	Differential Quadrature Method
FDM	Finite Difference Method
FFT	Fast Fourier Transform
GITT	Generalized Integral Transform Technique
HPM	Homotopy Perturbation Method
IMSL	International Mathematics and Statistics Library

frequency of pipe conveying fluid with different boundary conditions. Li et al. (2011) analyzed free vibration of multi-span pipe conveying fluid by dynamic stiffness method. Zhai et al. (2011) analyzed the dynamic response of pipeline conveying fluid under random excitation.

For numerical simulation of dynamic response of a beam or pipe, many different methods have been applied. Galerkin method is used widely to deal with this linear differential equation problems, see Lopes et al. (2002), Wadham-Gagnon et al. (2007), Modarres-Sadeghi et al. (2007) and Huang et al. (2010). Besides, many other numerical methods have been proposed, such as differential transformation method (DTM) implemented by Ni et al. (2011) to analyze vibration of pipes conveying fluid, precise integration method (PIM) performed by Liu and Xuan (2010) to analyze supported pipes conveying pulsating fluid, as well as homotopy perturbation method (HPM) (Xu et al., 2010) and differential quadrature method (DQM) (Lin et al., 2007; Qian et al., 2009). However, there are no previous study endeavored to perform vibration analysis of a clamped–clamped pipe conveying fluid based on generalized integral transform technique (GITT) approach. This approach, with its intrinsic characteristic of finding solutions with automatic global error control (Cotta, 1993, 1998; Cotta and Mikhailov, 1997), opened up an alternative perspective

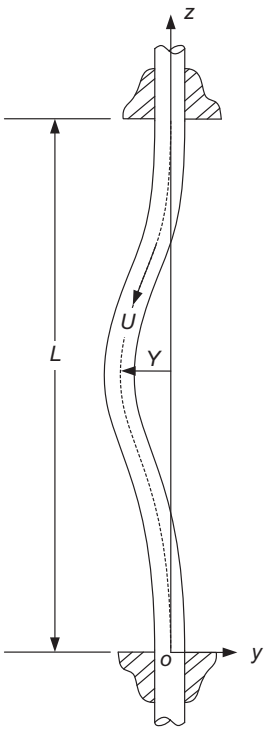

Fig. 1. Pipe conveying fluid with clamped–clamped boundary condition.

in benchmarking and covalidation for such dynamic response problems. Ma et al. (2006) applied GITT to solve a transverse vibration problem of an axial moving string, An and Su (2011) performed GITT to analyze dynamic response of clamped axially moving beams, and convergence behavior of integral transform solution was examined. At the present stage, GITT methodology was already successfully employed in the solution of bending problem of clamped orthotropic rectangular plates (An et al., 2011). The resulting system of transformed functions then offered an ordinary differential equation system as a boundary value problem, due to the parabolic nature of the modelling equations. Following the same line of research, the present work is thus aimed at utilizing the ideas in GITT methodology to construct a hybrid analytical–numerical solution, now for dynamic response of a clamped–clamped pipe conveying fluid. By adopting the same fourth-order eigenvalue problem, the transformed functions system results in an initial value problem to be numerically solved along the axial coordinate. The main purposes are: (1) computation of deflection and natural frequencies at several modes for various values of internal flow velocity and mass ratio, following a thorough convergence analysis of eigenfunction expansions; (2) critical comparisons with earlier published works for a covalidation against the present GITT results. This contribution will benefit the dynamic analysis of flow-induced vibrations on the design and maintenance of nuclear power plants.

2. Analysis

Consider an elastic pipe conveying fluids of a constant velocity U, as shown in Fig. 1. If gravitational forces, internal damping, externally imposed tension and pressurization effects are neglected, the linear equation of transverse motion $Y(Z,T)$ is given by Lee and Mote (1997a,b)

$$(m_f + m_p)\frac{\partial^2 Y}{\partial T^2} + 2m_f\frac{\partial^2 Y}{\partial Z\partial T} + m_f U^2\frac{\partial^2 Y}{\partial Z^2} + EI\frac{\partial^4 Y}{\partial Z^4} = 0, \quad Z \in (0, L), \tag{1}$$

where m_f and m_p are mass densities of the fluid and pipe, L is the length of the pipe, and EI is the flexural stiffness of the pipe. Introducing the following dimensionless variables

$$y=\frac{Y}{L},\quad z=\frac{Z}{L},\quad t=\frac{EI}{(m_f+m_p)}\frac{T}{L^2},\quad u=\sqrt{\frac{m_f}{EI}}UL,\quad \beta=\frac{m_f}{m_f+m_p}. \tag{2}$$

Eq. (1) can be written in dimensionless form as

$$\frac{\partial^2 y}{\partial t^2}+2\sqrt{\beta}u\frac{\partial^2 y}{\partial z\partial t}+u^2\frac{\partial^2 y}{\partial z^2}+\frac{\partial^4 y}{\partial z^4}=0,\qquad z\in(0,1). \tag{3}$$

The dimensionless boundary conditions are given as follows:

$$y(0,t)=0,\quad y(1,t)=0,\quad \frac{\partial y(0,t)}{\partial z}=0,\quad \frac{\partial y(1,t)}{\partial z}=0 \tag{4}$$

with initial conditions defined as follows:

$$y(z,0)=0,\quad \frac{\partial y(z,0)}{\partial t}=O(10^{-3})\quad \text{random noise}, \tag{5}$$

where $O(10^{-3})$ represents a random noise. These initial conditions are usually adopted to analyze dynamic transverse vibration of a slender pipe, see Violette et al. (2007).

3. Integral transform solution

Following the ideas in GITT, the next step is that of selecting eigenvalue problems and proposing eigenfunction expansions. The eigenvalue problem for transverse displacement $y(z,t)$ is chosen as expression (6):

$$\frac{d^4\phi_i(z)}{dz^4}=\lambda_i^4\phi_i(z),\quad 0<z<1 \tag{6}$$

with the following boundary conditions

$$\phi_i(0)=0,\quad \phi_i(1)=0,\quad \frac{d\phi_i(0)}{dz}=0,\quad \frac{d\phi_i(1)}{dz}=0, \tag{7}$$

where $\phi_i(z)$ is the eigenfunction of problem (6), λ_i is the corresponding eigenvalue, they satisfy the following orthogonality property

$$\int_0^1 \phi_i(z)\phi_j(z)\,dz=\delta_{ij}N_i \tag{8}$$

with $\delta_{ij}=0$ for $i\neq j$, and $\delta_{ij}=1$ for $i=j$. The norm, or normalization integral, is written as

$$N_i=\int_0^1 \phi_i^2(z)\,dz. \tag{9}$$

The selection of eigenfunction is computed based on the auxiliary eigenvalue problem with the boundary condition satisfied, even for some complex cases (Su, 2006). Then problem (6) is readily solved analytically to yield the eigenfunction

$$\phi_i(z)=\begin{cases}\dfrac{\cos[\lambda_i(x-0.5)]}{\cos(\lambda_i/2)}-\dfrac{\cosh[\lambda_i(x-0.5)]}{\cosh(\lambda_i/2)} & \text{for } i \text{ odd},\\ \dfrac{\sin[\lambda_i(x-0.5)]}{\sin(\lambda_i/2)}-\dfrac{\sinh[\lambda_i(x-0.5)]}{\sinh(\lambda_i/2)} & \text{for } i \text{ even},\end{cases} \tag{10a,b}$$

where the eigenvalues are obtained from the transcendental equations:

$$\tanh(\lambda_i/2)=\begin{cases}-\tan(\lambda_i/2) & \text{for } i \text{ odd},\\ \tan(\lambda_i/2) & \text{for } i \text{ even}.\end{cases} \tag{11}$$

The eigenvalue problem (6) allows definition of the following integral transform pair

$$\begin{cases}\bar{y}_i(t)=\displaystyle\int_0^1 \tilde{\phi}_i(z)y(z,t)\,dz, & \text{transform}\\ y(z,t)=\displaystyle\sum_{i=1}^{\infty}\tilde{\phi}_i(z)\bar{y}_i(t), & \text{inversion},\end{cases} \tag{12a,b}$$

where $\tilde{\phi}_i(z)$ is the normalized eigenfunction

$$\tilde{\phi}_i(z)=\frac{\phi_i(z)}{N_i^{1/2}}. \tag{13}$$

Now, the next step is thus to accomplish the integral transformation of the original partial differential system. For this purpose, Eq. (6), followed by the boundary conditions given by Eq. (7), are multiplied by $\int_0^1 \tilde{\phi}_i(z)\,dz$, integrated over the domain in z [0,1], and the inverse formula given by Eq. (12b) is employed. After the usual manipulations, the following coupled ordinary differential system results, for the calculation of the transformed $\bar{y}(t)$:

$$\frac{d^2\bar{y}_i(t)}{dt^2}+2\sqrt{\beta}u\sum_{j=1}^{\infty}A_{ij}\frac{d\bar{y}_i(t)}{dt}+u^2\sum_{j=1}^{\infty}B_{ij}\bar{y}_i(t)+\lambda_i^4\bar{y}_i(t)=0,$$
$$i=1,2,3,\ldots, \tag{14}$$

where the coefficients of the ordinary differential system are given by the following expressions:

$$A_{ij}=\int_0^1 \tilde{\phi}_i(z)\frac{d\tilde{\phi}_j(z)}{dz}\,dz,\quad B_{ij}=\int_0^1 \tilde{\phi}_i(z)\frac{d^2\tilde{\phi}_j(z)}{dz^2}\,dz. \tag{15}$$

The boundary conditions are naturally satisfied by the eigenfunctions. The initial conditions are also integral transformed to eliminate the spatial coordinate, yielding

$$\bar{y}_i(0)=0,\quad \frac{d\bar{y}_i(0)}{dt}=\int_0^1 \tilde{\phi}_i(z)\frac{\partial y(z,0)}{\partial t}\,dz,\quad i=1,2,3,\ldots \tag{16}$$

System (14) is now in an appropriate form for numerical solution through dedicated subroutines for initial value problems. The subroutine DIVPAG from IMSL Library (IMSL, 2003) is well tested and capable of handling such problems, offering automatic accuracy control, and for this problem the error tolerance 10^{-6} is selected. For computational purpose, the expansions are then truncated to N orders, so as to reach the user established accuracy target in final solution. The related coefficients given by Eq. (15) are also handled through IMSL Library. Once $\bar{y}_i(t)$ have been numerically evaluated, the analytical inversion formula (12b) is recalled to recover the dimensionless function $\tilde{y}(z,t)$.

4. Results and discussion

The typical time histories and response frequencies are shown in Fig. 2, with dimensionless parameters $u=4.5$, $\beta=1.0$, and truncation order $N=64$. The first column is dimensionless time history of y of the whole run at 5 equidistant space interval along the pipe, the second column is dimensionless time history in a interval $t\in[15, 17]$, the third column is the spectral analysis of second column. As shown in the first column, the vibration of the displacement keeps in long-term stability, and the second column demonstrated more clearly a fairly stable vibration. Several peaks of vibration dimensionless frequency appeared in spectral analysis, which indicates the mode shape have multi-mode contributions.

The convergence behavior of integral transform solution is examined for increasing truncation orders $N=4, 8, 16, 32$*and*64, the instantaneous deflections at dimensionless time $t=11$ are shown in

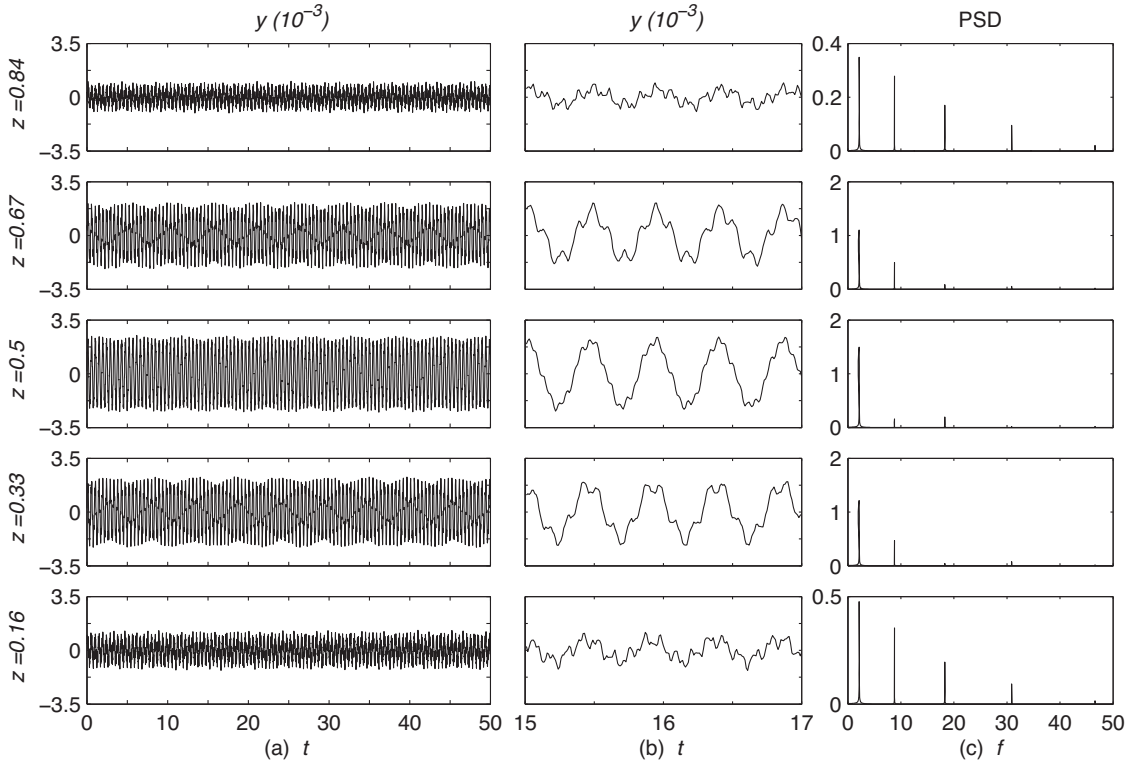

Fig. 2. Time history of simulation at $N = 64$, $u = 4.5$, $\beta = 1.0$. First column: dimensionless time history of transverse dimensionless deflection of the whole run at 5 equidistant space interval along the pipe; second column: dimensionless time history in a dimensionless time interval $t \in [15, 17]$; third column: spectral analysis of second column.

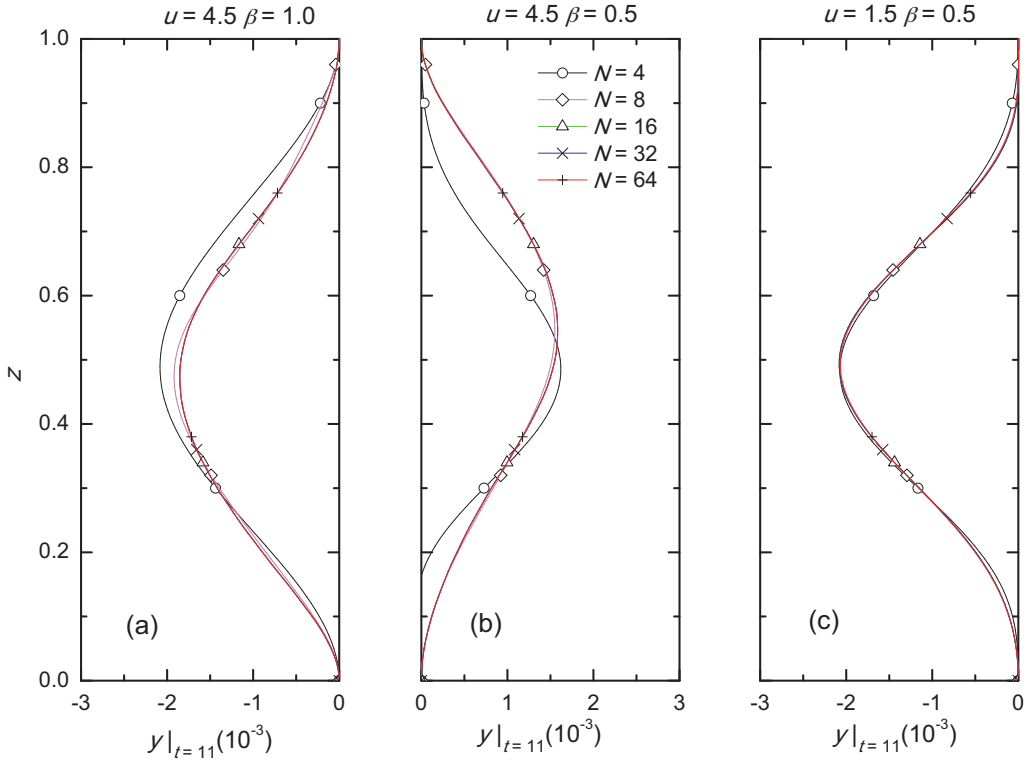

Fig. 3. GITT solutions with different truncation orders N for the dimensionless transverse deflection $y(z, t)$ at dimensionless time $t = 11$: (a) $u = 4.5$, $\beta = 1.0$; (b) $u = 4.5$, $\beta = 0.5$; (c) $u = 1.5$, $\beta = 0.5$.

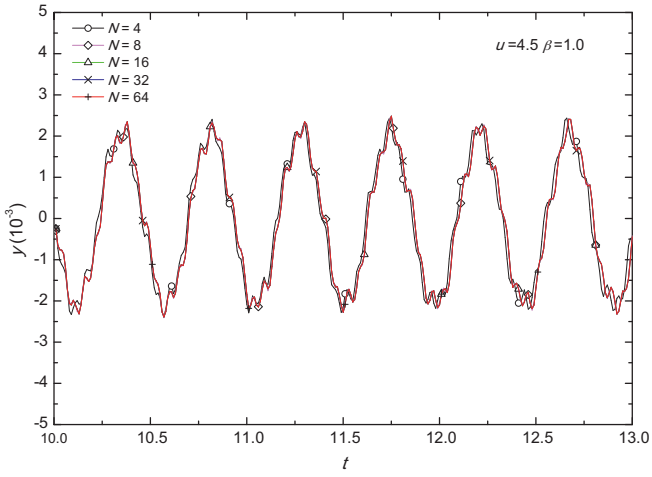

Fig. 4. GITT solutions with different truncation orders N for dimensionless time history $y(z, t)$ at $u = 4.5$, $\beta = 1.0$.

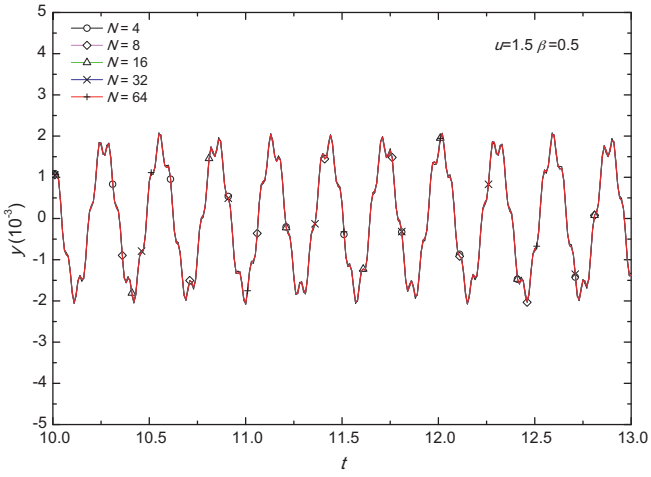

Fig. 6. GITT solutions with different truncation orders N for dimensionless time history $y(z, t)$ at $u = 1.5$, $\beta = 0.5$.

Fig. 3 with a combination of dimensionless flow velocity $u = 1.5, 4.5$ and mass ratio $\beta = 0.5, 1.0$. It can be observed that when $N \geqslant 16$, GITT solutions present a perfect convergence in the plots where these lines are nearly overlapped. Figs. 4–6 illustrate the convergence of dimensionless time trace in an interval $t \in [10, 13]$ with a combination of $u = 1.5, 4.5$ and $\beta = 0.5, 1.0$. It is noticed that the convergence is quite favorable. However, it should be pointed out that very low truncation orders may not capture actual displacement, such as the one in Fig. 3 with $N = 4$ and 8.

From FFT analysis shown in the third column of Fig. 2, the multi-mode contribution is captured. It is convenient to perform modal analysis by GITT since the solution is in form of eigenfunction expansions. Fig. 7 shows the mode contribution from 1 to 5 at $u = 4.5$, $\beta = 1.0$, with truncation order $N = 64$. It is clearly seen that the maximum deflections decreases when the mode number increases, and the deflection at mode 1 has a same vibration amplitude scale with the original one, which means the original deflections are dominated by mode 1, confirmed also by the power energy of FFT analysis shown in Fig. 2. Actually, the vibration amplitude approaches to 0 when truncation term N approaches to infinity, illustrating the excellent convergent behavior.

Figs. 8 and 9 present modal separation of dimensionless time trace in an interval $t \in [15, 17]$ and $u = 4.5$, $\beta = 1.0$, truncation order $N = 64$, at spanwise position $z = 0.5$ and 0.16, respectively. It depicts

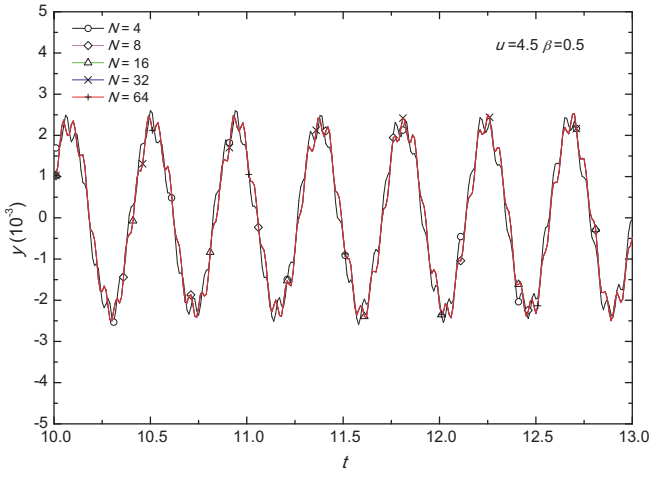

Fig. 5. GITT solutions with different truncation orders N for dimensionless time history $y(z, t)$ at $u = 4.5$, $\beta = 0.5$.

that mode 2 and 4 have zero amplitudes when $z = 0.5$, which can be verified in the Fig. 8, since $z = 0.5$ is the midpoint which keeps still at mode 2 and 4. The second column shows the clear dominated dimensionless frequencies of each mode. When $z = 0.16$, spectral analysis presents clearly the multi-mode contributions, and natural frequency at each mode can be easily obtained.

We now proceed towards the validation of proposed approach against previously reported results in literature. Here, we defined dimensionless natural angular frequency $\omega = 2\pi f$, where f is dimensionless natural frequency. A comparison of variations of ω at mode 1–3 with increasing u between GITT and theory (Païdoussis, 1998) are illustrated by Fig. 10, which shows that ω decreases with the increasing of u, and ω at mode 1 is approaching 0 as u is approaching 2π. The value 2π is defined as a critical internal flow velocity u_{cd} of the pipe with a clamped–clamped boundary condition by theoretical analysis (Païdoussis, 1998), when $u < u_{cd}$, the eigenfrequencies are all purely real, whilst for $u > u_{cd}$ those associated with the first mode are purely imaginary, which means the system loss stability. Our GITT solution presents a divergence when $u > u_{cd}$, which verifies the critical velocity. Besides, it can be seen that numerical results obtained in present work agree very well with theoretical predictions by Païdoussis (1998).

The maximum vibration deflection increases as the flow velocity increases, which is verified by experiment Guo and Lou (2008). However, the variation of deflection versus flow velocity was not qualitatively and quantitatively evaluated. GITT is used here since it is convenient to analyze dynamic response of pipe conveying fluid both at frequency and time domain. Fig. 11 presents deflection ratio y_M/y_M^* versus u at $\beta = 0.1$, where y_M and y_M^* denote maximum deflections when $u \neq 0$ and $u = 0$, respectively. It is seen that when u increases from 0 to 5, y_M/y_M^* increases slowly from 1 to 1.5, but when it increases from 5 and approaches to critical velocity 2π, y_M/y_M^* increases exponentially from 1.5 to 6. This phenomenon depicts that the influence of internal flow velocity has a dramatical increase when u approaches the critical flow velocity, which should be careful in pipe design.

Finally, we consider the influence of mass ratio β on dynamic responses of pipe conveying fluid. Païdoussis (1998) evaluated the influence of mass ratio on the critical velocity to yield a map of different kinds of instabilities predicted by linear theory for clamped–clamped pipes. However, the maximum vibration deflection and natural angular frequencies under different mass ratios are also valuable to engineers. Fig. 12 presents y_M/y_M^* versus β, at $u = 4.5$. It is observed that the y_M/y_M^* decreases linearly from 1 to 0.865 when β increases from 0 to 1. The variation of dimensionless

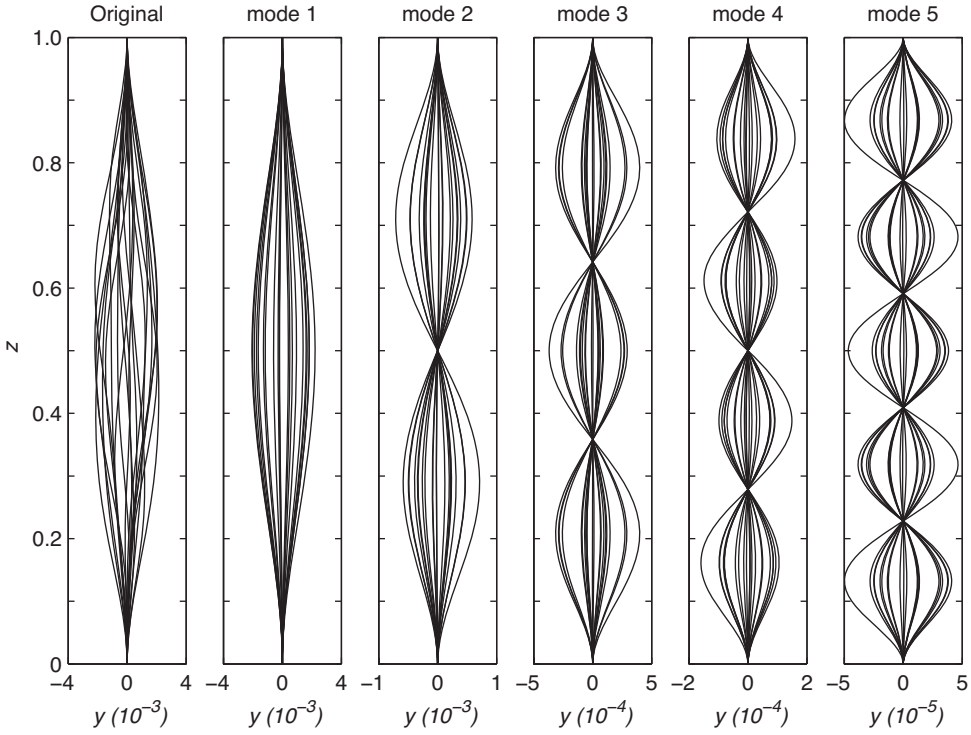

Fig. 7. Mode separation of instantaneous deflections with dimensionless time interval $\Delta t = 1$ at $u = 4.5$, $\beta = 1.0$, truncation order $N = 64$.

natural angular frequencies at mode 1–5 ($\omega_1, \omega_2, \omega_3, \omega_4, \omega_5$) versus mass ratio is shown in Table 1. It is interesting to notice that dimensionless natural angular frequency at first mode (ω_1) decreases monotonically when β increases from 0 to 1, while those at mode 2–5 ($\omega_2, \omega_3, \omega_4, \omega_5$) increase monotonically when β increases from 0 to 1.

From the excellent agreement of the present results with previously theory shown above, the solution of GITT could be considered as the exact solution. To clarify the so-called "exact solution", it is necessary to make final remarks about the nature of the proposed approach. Each term of $\tilde{\phi}_i(z)$ and $\bar{y}_i(t)$ satisfies boundary conditions, besides, there is no approximation involved in the analytical

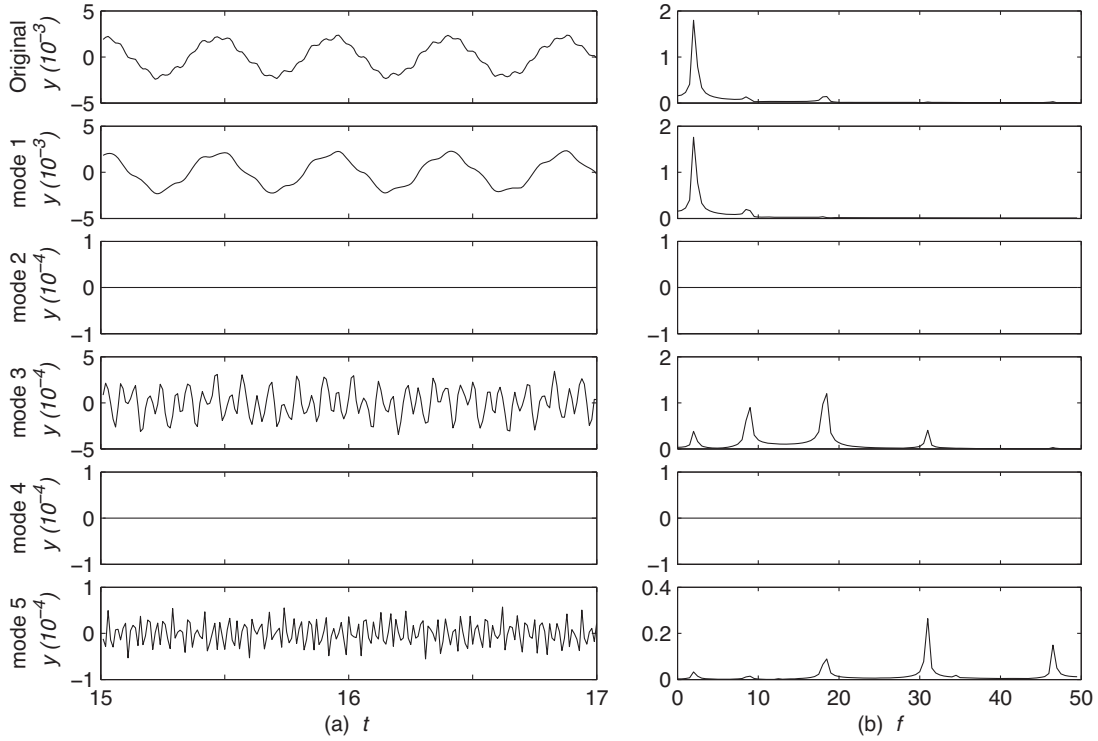

Fig. 8. Mode separation of dimensionless time history $y(z, t)$ in a dimensionless time interval $t \in [15, 17]$ at $u = 4.5$, $\beta = 1.0$, truncation order $N = 64$, spanwise position $z = 0.5$.

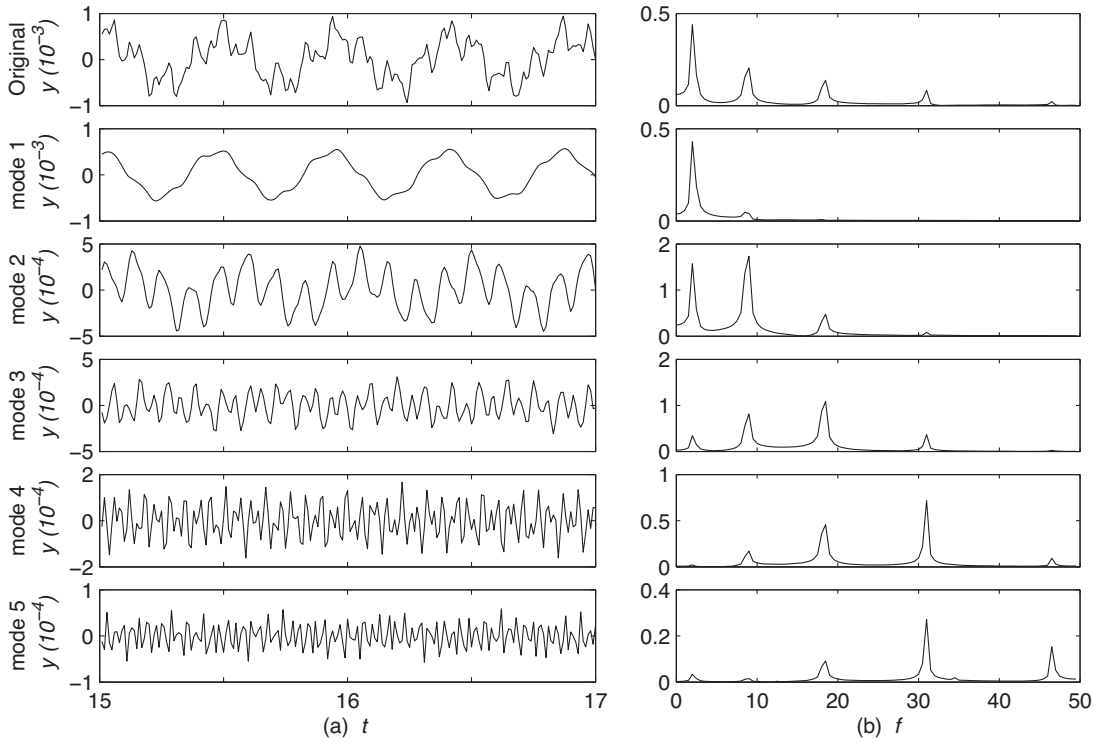

Fig. 9. Mode separation of dimensionless time history $y(z, t)$ in a dimensionless time interval $t \in [15, 17]$ at $u = 4.5$, $\beta = 1.0$, truncation order $N = 64$, spanwise position $z = 0.16$.

derivation of GITT approach, the problem solution represented by the summation of a rapidly converging infinite series (12b) simultaneously satisfies the governing differential equation (3) and the boundary conditions (4). In real calculations, the derived series solution needs to be truncated somewhere for computational evaluation. In other words, the problem can only be dealt with through finite series instead of the infinite range in the analytical formulation. Therefore, the exact solution can be characterized as a truncated series solution with the desired precision, which can be achieved by controlling every numerical step with prescribed accuracy. This automatic and straightforward global error control procedure makes GITT particularly suitable for benchmarking purposes of such dynamic analysis of structures.

However, there are some other good methods, such as the time step integration method. There have been tremendous researches on the method of direct integration algorithms, including the Runge-Kutta method, the Houbolt method, the Newmark method, the Wilson method, the central difference method, etc. They are all FDM (Finite Difference Method) approaches, but the finite difference approximation is always accompanying with error, and has also numerical problem including stiff, stability etc., not so ideal. For instance, a good implementation of a Runge-Kutta method requires an efficient step size control. In principle, one tries to choose the step size in each step such that the new local error does not exceed a

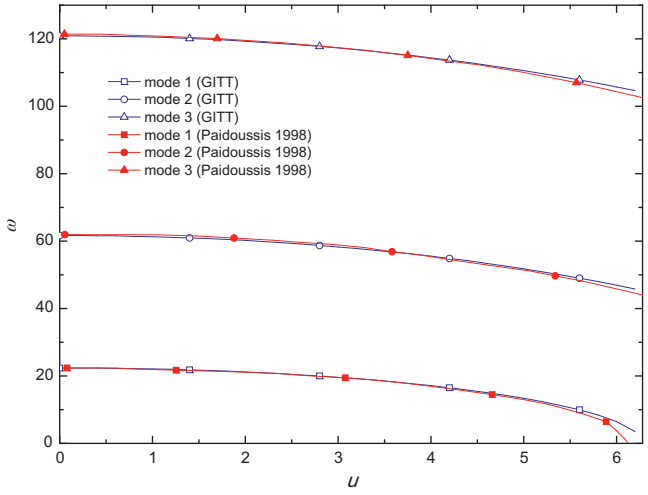

Fig. 10. Dimensionless natural angular frequency ω at mode 1–3 versus dimensionless flow velocity u, at $\beta = 0.1$.

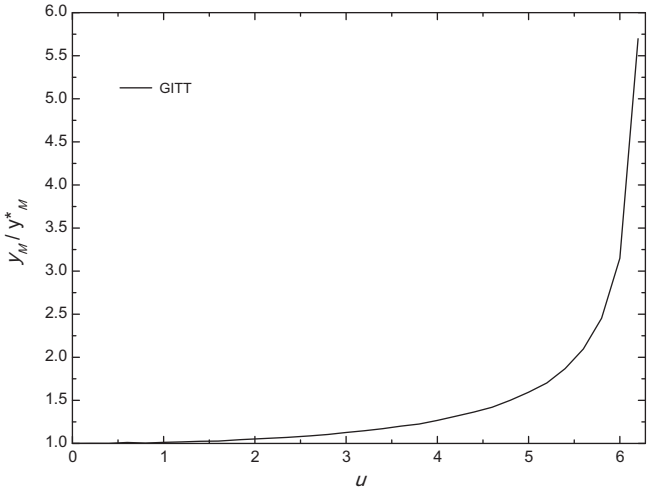

Fig. 11. Deflection ratio y_M/y_M^* versus dimensionless flow velocity u, at $\beta = 0.1$.

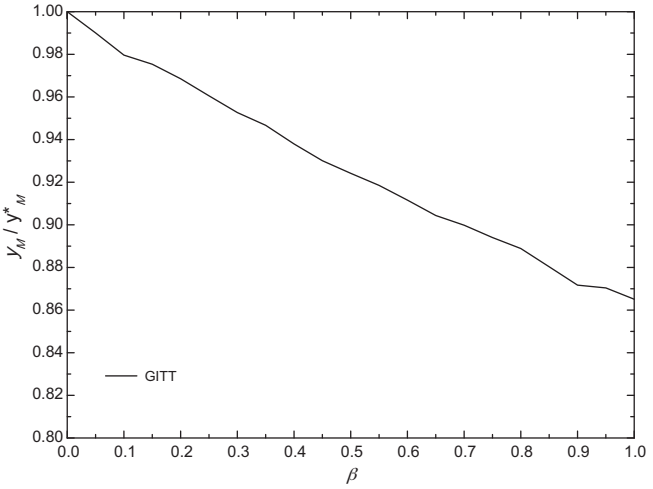

Fig. 12. Deflection ratio y_M/y_M^* versus mass ratio β, at $u = 4.5$.

Table 1
Dimensionless natural angular frequencies ω_1, ω_2, ω_3, ω_4, ω_5 versus mass ratio β, at $u = 4.5$.

β	ω_1	ω_2	ω_3	ω_4	ω_5
0.05	15.6182	53.6764	112.4690	191.0986	289.6548
0.10	15.4387	53.7661	112.5588	191.2781	289.8344
0.15	15.3489	53.9456	112.7383	191.4576	290.0139
0.20	15.1694	54.0354	112.9178	191.6372	290.1934
0.25	15.0796	54.1252	113.0076	191.8167	290.3729
0.30	14.9899	54.2149	113.1871	191.9064	290.5524
0.35	14.8104	54.3944	113.2769	192.0860	290.7320
0.40	14.7206	54.4842	113.4564	192.2655	290.9115
0.45	14.6308	54.5740	113.5461	192.4450	291.0910
0.50	14.4513	54.5740	113.7257	192.5347	291.1808
0.55	14.3616	54.6637	113.8154	192.7143	291.3603
0.60	14.2718	54.7535	113.9052	192.8938	291.5398
0.65	14.1820	54.8432	114.0847	193.0733	291.7193
0.70	14.0923	54.9330	114.1745	193.1631	291.8988
0.75	14.0025	54.9330	114.2642	193.3426	292.0784
0.80	13.9128	55.0228	114.4437	193.5221	292.2579
0.85	13.7332	55.0228	114.5335	193.6119	292.4374
0.90	13.6435	55.1125	114.6233	193.7914	292.5272
0.95	13.5537	55.1125	114.8028	193.8811	292.7067
1.00	13.4640	55.2023	114.8925	194.0607	292.8862

prescribed tolerance. Unfortunately, explicit Runge-Kutta methods are generally unsuitable for the solution of stiff equations because their region of absolute stability is small. This issue is especially important in the solution of partial differential equations. The instability of explicit Runge-Kutta methods motivates the development of implicit methods, but the computational costs would be significantly increased.

5. Conclusions

The integral transform method was applied to obtain a hybrid numerical–analytical solution of dynamic response of a clamped–clamped pipe conveying fluid. The analysis of convergence behavior and comparison with theoretical results were performed. Excellent agreement of the present results with previously theory demonstrates the convenience and exceptional computational performance of the proposed methodology. Numerical results illustrate the dynamic response is dominated by mode 1 through modal separation analysis. The deflection ratio increases as the flow velocity increases, and decreases as the mass ratio increases. Meanwhile, the natural angular frequency decreases monotonically at first mode but increases monotonically at mode 2–5 when the mass ratio increases.

Acknowledgments

The authors acknowledge gratefully CNPq, CAPES and FAPERJ of Brazil, the National Basic Research Program of China (973 Program) Grant No. 2011CB013702 and the Natural Science Foundation of China Grant No. 50979113 for the financial support to this research.

References

An, C., Gu, J.-J., Su, J., 2011. Integral transform solution of bending problem of clamped orthotropic rectangular plates. In: International Conference on Mathematics and Computational Methods Applied to Nuclear Science and Engineering (M&C 2011), Rio de Janeiro, RJ, Brazil, May 8–12.
An, C., Su, J., 2011. Dynamic response of clamped axially moving beams: integral transform solution. Appl. Math. Comput. 218 (2), 249–259.
Cotta, R.M., 1993. Integral Transforms in Computational Heat and Fluid Flow. CRC Press, Boca Raton, USA.
Cotta, R.M., 1998. The Integral Transform Method in Thermal and Fluids Sciences and Engineering. Begell House, New York, USA.
Cotta, R.M., Mikhailov, M.D., 1997. Heat Conduction – Lumped Analysis, Integral Transforms, Symbolic Computation. Wiley/Interscience, UK.
Guo, H.Y., Lou, M., 2008. Effect of internal flow on vortex-induced vibration of risers. J. Fluids Struct. 24 (4), 496–504.
Huang, Y.-M., Liu, Y.-S., Li, B.-H., Li, Y.-J., Yue, Z.-F., 2010. Natural frequency analysis of fluid conveying pipeline with different boundary conditions. Nucl. Eng. Des. 240 (3), 461–467.
Ibrahim, R.A., 2010. Overview of mechanics of pipes conveying fluids. Part I. Fundamental studies. J. Pressure Vessel Technol.: Trans. ASME 132 (3).
Ibrahim, R.A., 2011. Mechanics of pipes conveying fluids. Part II. Applications and fluid elastic problems. J. Pressure Vessel Technol.: Trans. ASME 133 (2).
IMSL, 2003. IMSL Fortran Library version 5.0, MATH/LIBRARY, vol. 2. Visual Numerics, Inc., Houston, TX.
Kang, M.-G., 2010. The influence of rotary inertia of concentrated masses on the natural vibrations of a clamped-supported pipe conveying fluid. Nucl. Eng. Des. 196, 461–467.
Lee, S.Y., Mote, C.D., 1997a. A generalized treatment of the energetics of translating continua. 1. Strings and second order tensioned pipes. J. Sound Vibration 204 (5), 717–734.
Lee, S.Y., Mote, C.D., 1997b. A generalized treatment of the energetics of translating continua. 2. Beams and fluid conveying pipes. J. Sound Vibration 204 (5), 735–753.
Li, B.-h., Gao, H.-s., Zhai, H.-b., Liu, Y.-s., Yue, Z.-f., 2011. Free vibration analysis of multi-span pipe conveying fluid with dynamic stiffness method. Nucl. Eng. Des. 241 (3), 666–671.
Lin, W., Qiao, N., Huang, Y., 2007. Dynamical behaviors of a fluid-conveying curved pipe subjected to motion constraints and harmonic excitation. J. Sound Vibration 306 (3–5), 955–967.
Liu, L., Xuan, F., 2010. Flow-induced vibration analysis of supported pipes conveying pulsating fluid using precise integration method. Math. Problems Eng.
Lopes, J.L., Païdoussis, M.P., Semler, C., 2002. Linear and nonlinear dynamics of cantilevered cylinders in axial flow. Part 2: The equations of motion. J. Fluids Struct. 16 (6), 715–737.
Ma, J.-K., Su, J., Lu, C.-H., Li, J.-M., 2006. Integral transform solution of the transverse vibration of an axial moving string. J. Vibration, Measur. Diagn. 26 (117), 104–107.
Modarres-Sadeghi, Y., Semler, C., Wadham-Gagnon, M., Païdoussis, M.P., 2007. Dynamics of cantilevered pipes conveying fluid. Part 3. Three-dimensional dynamics in the presence of an end-mass. J. Fluids Struct. 23 (4), 589–603.
Ni, Q., Zhang, Z.L., Wang, L., 2011. Application of the differential transformation method to vibration analysis of pipes conveying fluid. Appl. Math. Comput. 217 (16), 7028–7038.
Païdoussis, M.P., 1998. Fluid–Structure Interactions: Slender Structures and Axial Flow, vol. 1. Academic Press, London.
Païdoussis, M.P., Grinevich, E., Adamovic, D., Semler, C., 2002. Linear and nonlinear dynamics of cantilevered cylinders in axial flow. Part 1. Physical dynamics. J. Fluids Struct. 16 (6), 691–713.
Païdoussis, M.P., Semler, C., Wadham-Gagnon, M., Saaid, S., 2007. Dynamics of cantilevered pipes conveying fluid. Part 2. Dynamics of the system with intermediate spring support. J. Fluids Struct. 23 (4), 569–587.
Qian, Q., Wang, L., Ni, Q., 2009. Instability of simply supported pipes conveying fluid under thermal loads. Mech. Res. Commun. 36 (3), 413–417.
Semler, C., Lopes, J.L., Augu, N., Païdoussis, M.P., 2002. Linear and nonlinear dynamics of cantilevered cylinders in axial flow. Part 3. Nonlinear dynamics. J. Fluids Struct. 16 (6), 739–759.

Sinha, J.K., Rao, A.R., Sinha, R.K., 2005. Prediction of flow-induced excitation in a pipe conveying fluid. Nucl. Eng. Des. 235 (5), 627–636.

Su, J., 2006. Exact solution of thermal entry problem in laminar core-annular flow of two immiscible liquids. Chem. Eng. Res. Des. 84 (11), 1051–1058.

Violette, R., de Langre, E., Szydlowski, J., 2007. Computation of vortex-induced vibrations of long structures using a wake oscillator model: comparison with DNS and experiments. Comput. Struct. 85 (11–14), 1134–1141.

Wadham-Gagnon, A., Païdoussis, M.P., Semler, C., 2007. Dynamics of cantilevered pipes conveying fluid. Part 1. Nonlinear equations of three-dimensional motion. J. Fluids Struct. 23 (4), 545–567.

Xu, M.R., Xu, S.P., Guo, H.Y., 2010. Determination of natural frequencies of fluid-conveying pipes using homotopy perturbation method. Comput. Math. Appl. 60 (3), 520–527.

Zhai, H.-B., Wu, Z.-Y., Liu, Y.-S., Yue, Z.-f., 2011. Dynamic response of pipeline conveying fluid to random excitation. Nucl. Eng. Des. 241 (8), 2744–2749.